Layout and Manage of Micro-Grid Fed through Renewable Power Generating Sources

Anoj Kumar Singh[1] Saurav Kumar[2]
[1,2]Lecturer
[1]Department of Physics [2]Department of Electronics Engineering
[1,2]Government Polytechnic Chhapra, Bihar, India

Abstract— This paper offers a manage of a micro-grid at an remoted region fed from wind and solar based totally hybrid energy sources. The machine used for wind power conversion is doubly fed induction generator (DFIG) and a battery financial institution is attached to a not unusual dc bus of them. A sun photovoltaic (pv) array is used to transform sun electricity, that's evacuated on the not unusual dc bus of DFIG the use of a dc-dc improve converter in a cost effective manner. The voltage and frequency are managed via an oblique vector control of the road facet converter, that's included with droop traits. It alters the frequency set factor primarily based at the power level of the battery, which slows down over charging or discharging of the battery. The device is likewise able to paintings whilst wind strength source is unavailable. Each wind and sun power blocks, have maximum power point monitoring (MPPT) of their manipulate algorithm. The gadget is designed for complete automatic operation taking attention of all of the sensible situations. The machine is likewise furnished with a provision of outside energy aid for the battery charging with none extra requirement. A simulation version of gadget is evolved in matlab surroundings and simulation consequences are supplied for numerous conditions e.G. Unviability of wind or sun energies, unbalanced and nonlinear masses, low state of fee of the battery. In the end a prototype of the device is carried out the usage of a five kw solar pv array simulator and a 3.7 kw wound rotor induction machine and experimental results are produced to reaffirm the theoretical version and layout.

Keywords: DFIG, Vector Control, Wind Energy; Power Quality, Solar PV Energy, Micro-grid, Battery Energy Storage System, Renewable Energy System

I. INTRODUCTION

There are many remote locations in the world, which don't have access to electricity. There are also many places, which are connected to the grid, however, they don't receive electricity for up to 10-12 hours in the day and as a result of it, economic activities of inhabitants suffer. Many of such places are rich in renewable energy (RE) sources such as wind, solar and bio-mass. An autonomous generation system utilising locally available RE sources, can greatly reduce the dependency on the grid power, which is predominantly fossil power. Wind and solar energy sources, are more favorite than bio-mass based system as latter is susceptible to supply chain issue. However, wind and solar energies suffer from high level of power variability, low capacity utilization factor combined with unpredictable nature. As a result of these factors, firm power cannot be guaranteed for autonomous system. While the battery energy storage (BES) can be helpful of lowering power fluctuation and increasing predictability, utilisation factor can be increased by operating each energy source at optimum operating point. The optimum operating point also called as maximum power point tracking (MPPT), requires regulation of the operating point of wind energy generator and solar PV (Photovoltaic) array in term of speed and voltage to extract maximum electrical energy from input resource. The MPPT can be achieved by power electronics (PE) based control. PE based control can also help energy management for BES.

Many authors have reported autonomous solar PV systems [1-2] and autonomous wind energy systems [3-4]. However, autonomous system with only one source of energy, requires very large size of storage and associated PE components.

A hybrid energy system consisting of two or more type of energy sources, has ability to reduce the BES requirement and increases reliability. Wind and solar energies are natural allies for hybridization. Both have been known to be complementary to each other in daily as well as yearly pattern of the behavior. Acknowledging advantages of this combination, many authors have presented autonomous wind solar hybrid systems [5-10]. The most favorite machine for small wind power application, is permanent magnet synchronous generator [4-5]. It is possible to achieve gearless configuration with PMSG, however, it requires 100% rated converter in addition to costlier machine [11]. Some authors have also used wind solar hybrid system with a squirrel cage induction generator (SCIG) [6], Though SCIG has commercial edge regarding machine cost, however, the scheme doesn't have speed regulation required to achieve MPPT. Moreover, if the speed regulation is done, it requires full power rated converter.

A doubly fed induction generator (DFIG) as a generator is commonly used for commercial wind power generation and its applications, have been presented by many authors in their publications for autonomous application along with solar PV array [7-10]. DFIG may operate variable speed operation with lower power rated converters. However, to work the system as a micro-grid, the generated voltage should be balanced and THD (Total Harmonics Distortion), must be within requirement of IEEE-519 standard at no-load, unbalanced load as well as nonlinear load. Moreover, both the wind and solar energies sources should operate at MPPT. None of the authors, has reported all these issues. They have not presented performance parameters e.g. power quality, system efficiency etc. under the different operating conditions. Moreover, they also lack experimental verification.

This paper presents a micro-grid fed from wind and solar based renewable energy generating sources (REGS). DFIG is used for wind power conversion while crystalline solar photovoltaic (PV) panels are used to convert solar energy. The control of overall scheme, helps to provide

quality power to its consumers for all conditions e.g. no-load, nonlinear load and unbalanced loads. The controls of both generating sources, are equipped with MPPT. Emmanouil et al. [12] have proposed a droop based control system for micro-grid with the help of standalone battery converter. In the presented scheme, the droop characteristic is embedded in control of load side converter (LSC) of DFIG. This function varies the system frequency based on state of charge of the battery and slows down deep discharge and over-charge of the battery.

The DFIG in a proposed system, has also two voltage source converters (VSC). In addition to LSC, DFIG also has another VSC connected to rotor circuit termed as rotor side converter (RSC). The function of RSC is to achieve wind MPPT (W-MPPT). The solar PV system is connected to the DC bus through solar converter, which boosts the solar PV array voltage. With this configuration, the solar power can be evacuated in a cost effective way. This converter too is equipped with solar MPPT(S-MPPT) control strategy to extract maximum solar energy. In case of unavailabity of wind energy source and lower state of charge of the battery, the battery bank can be charged through the grid power or a diesel generator through the same RSC. With the help of the LSC, rated frequency and voltage at the load terminals, are maintained under following conditions.

- Varying amount of solar and wind powers.
- Unavailability of solar power or wind power.
- Loss of load or breakdown of the distribution system.
- Different types of loads as unbalanced and nonlinear loads.

It presents the design criteria of major components and control strategies for various converters. Finally it presents simulation results followed by experimental results obtained on a prototype developed in the laboratory.

II. SYSTEM COMPONENTS DESCRIPTION

A single line diagram of the proposed renewable energy generation system (REGS) fed micro-grid is shown in Fig. 1. The same has been designed for location having maximum power demand and average power demand of 15 kW and 5 kW, respectively. The rated capacity of both wind and solar energy block in REGS, is taken as 15 kW. The capacity utilisation factor of 20% is considered for both energy blocks, which is enough to provide full day energy requirement of the hamlet.

As shown in a schematic diagram, the wind energy source is isolated using a 3-pole breaker from the network in case of insufficient wind speed. The DC side of both RSC and LSC along with HV side of solar converter, is connected at the battery bank. RSC helps the wind energy system to run at the optimum rotation speed as required by W-MPPT algorithm. The LSC controls the network voltage and frequency. The energy flow diagram of the system is shown in Fig. 2.

The design methodology of major components of REGS, is shown in following sub-sections.

A. Wind Turbine and Gear

The wind turbine captures the kinetic energy of the wind and provides driving torque for DFIG. The value of captured mechanical power is given as,

$$P = 0.5c\,\pi\, r^2 \rho V^3 \qquad (1)$$

Here V_w, and r, are wind speed and radius of wind turbine respectively. C_p is the coefficient of performance of wind turbine and is mathematically derived as [13],

$$c\,(\lambda,\beta) = -0.002*\beta^{2.14} - 13.2)e \qquad (2)$$

0.73(lemda bar

Where

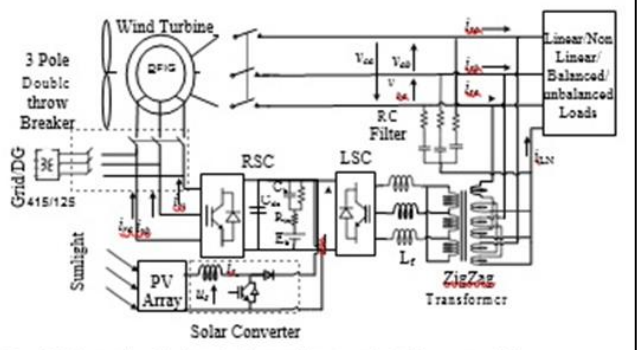

Fig. 1 Schematic of isolated micro-grid network fed by renewable energy source using battery storage

$$\frac{1}{\lambda_i} = \frac{1}{(\lambda + 0.08\beta)} - \frac{0.03}{\beta^3 + 1} \qquad (3)$$

λ and β are the tip speed ratio(TSR) and the turbine blade pitch angle, respectively.

TSR is related to the of the turbine speed ω_r, turbine radius r and wind speed V_w as,

$$\lambda = \omega_r\, r/(\eta_G V_W) \qquad (4)$$

$$\eta = \omega\, r/(\lambda^* V) \qquad (5)$$

where η_G is the turbine shaft gear ratio.

The rated capacity of wind generator used in proposed scheme is 15 kW at a rated wind speed (V_{wr}) of 9 m/s and rotational speed (ω_{rm}) of 198 rad/s. The optimum TSR (λ^*) and turbine radius, are taken 5.67 and 4.3 m, respectively. The control action maintains W-MPPT till the machine speed reaches ω_{rm}. Having known λ^*, V_{wr} and ω_{rm}, gear ratio η_G is determined from (5) as,

$\eta_G = (198 \times 4.3)/(5.67 \times 9) = 16.68$

B. DFIG

An external power flow in DFIG, is through both stator and rotor. Neglecting losses, at maximum wind speed, the nominal power of DFIG (P_e) is related to rated air gap power (P_{ag}) as

$$P_e = P_{ag}/(1+|s_{pmax}|)) \qquad (6)$$

S_{pmax} is the slip corresponding to the turbine speed, ω_{rm} and its value is -0.267. The speed range of DFIG is the speed corresponding to slip 0.3 to -0.267. Assuming air gap power(P_{ag}) equal to mechanical input power, the electrical power rating of the machine P_e corresponding to maximum input power, is {15/(1+0.267)} =11.83 kW. When the wind turbine is in service, the complete magnetising power requirement of machine is provided by

RSC. Hence 11.83 kW capacity of DFIG is adequate to convert mechanical power from 15 kW wind energy system to electrical energy. Taking additional margin due to electrical losses, a 12.5 kW machine is chosen, which detailed parameters, are given in Appendix A.

C. Transformer

The load and stator terminals are connected to the LSC through a zig-zag transformer, which also provides neutral for single phase loads at 415 V side. The maximum absolute value of rotor slip, is 0.3 and accordingly, the maximum rotor voltage V_{rmax} becomes 125 V(0.3×415 V). The voltage at the LV side of zig-zag transformer is also chosen to be equal to V_{rmax} Accordingly the transformer has a voltage ratio 415/125 V and its HV windings are connected to the stator and the load.

The zig-zag transformer should meet the combined kVA requirement of load as well as connected filters. Accordingly, a 20 kVA transformer is chosen, which is sufficient to transfer rated power along with meeting reactive power requirement of the connected loads and filters at peak demand.

D. Battery Sizing

The maximum operating slip of machine is 0.3. The DFIG speed corresponding to this slip is 110 rad/s. At this slip, the line voltage of rotor V_{rmax} become 125 V (415×0.3). The required DC bus voltage (V_{dc}) for PWM control is as,

$$\sqrt{V_{dc}} > \{2\,(2/3)V_L\}m_i \qquad (7)$$

V_L is the higher of the line voltage of low voltage (LV) side of the zig-zag transformer and the rotor voltage at highest slip. The maximum operating slip is 0.3 and accordingly the highest rotor voltage as well as LV side of zig-zag transformer is 125 V. The modulation index, m_i is chosen to be unity. Based on these inputs, the DC bus voltage V_{dc} required for functioning of PWM control must not be less than 204 V. In the presented scheme, V_{dc} is taken 240 V.

The proposed micro-grid is designed to provide load requirement of 5 kW without any generating source for an up to 12 hours. Taking additional 20% margin for energy losses during exchange of energy, the required battery storage capacity becomes 72 kWhr. At the DC bus voltage of 240 V, the Ampere-Hour (AH) rating of battery becomes 300 AH (72,000/240). This is achieved using 40 numbers of 12V, 150 AH lead acid batteries divided equally into two parallel circuits.

A lead acid battery bank can be safely operated between 2.25 V and 1.8 V per cell. This makes the maximum battery voltage V_{bmax} and minimum battery voltage V_{bmin} to be 270 V and 216 V, respectively. A battery bank can be assumed to a DC source with fictitious capacitor C_b, internal resistance R_{in} connected in series. In addition to it, another resistance R_b is connected across the battery to denote energy drain due to self discharge of battery.

C_b in series with the battery denotes voltage change due to charging and discharging. The value of C is determined as [14],

$$Cb=kWh \times 3600 \times 1000/\{0.5 \times(Vbmax^2-Vbmin^2)\} \qquad (8)$$

Substituting variables in (8), C_b is obtained 19753 F.

E. Solar PV System

The basic element of a solar PV system is the solar cell, which is based on the work of Rey-Boué et al [15]. The solar panels are configured such that the open circuit voltage of the solar string remains less than the lowest downstream voltage of solar converter or DC bus voltage, V_{dc}. The cell numbers (N_c) in a string, is a function of its DC voltage and cell open circuit voltage V_{occ} as,

$$N_c=V_{dcm}/V_{occ} \qquad (9)$$

The value of v_{occ} based on a typical commercially available cell characteristics and its value, is taken as 0.64 V. As evaluated in sub-section (D), the minimum battery voltage can fall down upto 216 V. Solar array voltage (u_s) can vary up to 3%, which is due to manufacturing tolerance of electrical quantities of module. Hence V_{dcm} is taken as 210 V and accordingly, the required numbers of cell, N_c as derived from comes to be 328 cells. To evenly distribute the cells in a standard configuration, 324 cells are taken, which are divided in 9 modules of 36 cells each. The ratio of V_{occ} to cell voltage at maximum power point (MPP), V_{mpc} for a typical module characteristic is 1.223. Accordingly, the module voltage at MPP becomes (V_{mpc} x 36) 18.83 V and u_s becomes 169.47 V.

At 15 kW solar array capacity, the cumulative string current at MPP becomes {15000/(9*18.83)}88.5 A. The number of string in the solar array is chosen to be 11, accordingly module current at MPP, I_{mp} becomes 8.04 A. The ratio of short circuit current I_{sc} to I_{mp} for a typical module is 1.081 and accordingly I_{sc} is taken as 8.69 A.

The detailed parameters used for modeling of solar energy block, are given in Table-I

F. High Pass Filter

To reduce voltage ripples, a high pass filter is used at stator terminal, which time constant should be less than fundamental frequency i.e. 20 ms. Moreover, it should be tuned half the switching frequency. The switching frequency is 10 kHz and accordingly the filter to be designed for 5 kHz. In the present scheme, a series RC filter consisting of 5 Ω resistance and 15 μF capacitance, is connected at the stator terminals of DFIG. The filter provides less than 5.43 Ω impedance for harmonic voltage having more than 5 kHz frequency.

III. CONTROL ALGORITHM

As shown in Fig.1, REGS consists of three converters, which control descriptions, are given as follows.

A. Control of Solar Converter

A solar converter, which is a boost type DC-DC converter used to evacuate solar power with embedded S- MPPT logic. It is based on incremental conductance method [16]. The S- MPPT through intelligent switching regulates u_s so as the solar system operates at MPP. The flow diagram of the MPPT algorithm is shown in Fig.3.

B. Control of LSC

Since the onshore wind turbine generates power only for 60-70% of the time, the system should be designed to work when no wind power is available. As shown in the control diagram in Fig. 4, i^*_{qs} consists of two components. The first

component, i_{qs1} corresponds to the power component of DFIG current when wind turbine is in operation. The second components I_{usd} corresponds to the power component drawn when stator of DFIG is not connected to the load terminal.

Open Circuit Voltage of PV cell, Vocc	0.64 V
Open circuit voltage of a module (V_{oc})	23.04 V
MPP voltage of PV cell, Vmpc	0.5223 V
MPP Voltage of module(V_{mp})	18.83 V
Short Circuit current of module(I_{sc})	8.69 A
MPP current of module (I_{mp})	8.04 A
Module Power Rating	151 Wp
μIsc	0.04 %/ ºC
μVoc	-0.36%/ ºC
PV Modules in the solar block	11 strings each having 9 PV modules.
String open circuit voltage, u_{soc}	207.36 V
Capacity of Solar PV System	15 kWp

Table 1: Technical Details of Solar Block

The direct component of current, i^*_{ds} corresponds to the reactive power requirement at the point of common interconnection of the generator and filter. The information of and i^*_{as} and i^*_{ds} provides the reference stator currents and help in maintaining the voltage and frequency through the indirect vector control as elaborated.

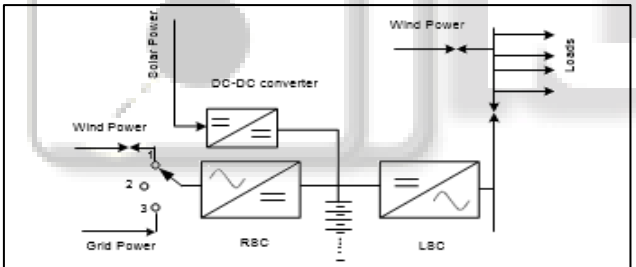

Fig. 2 Energy flow diagram of isolated micro-grid network fed by renewable energy source using battery storage

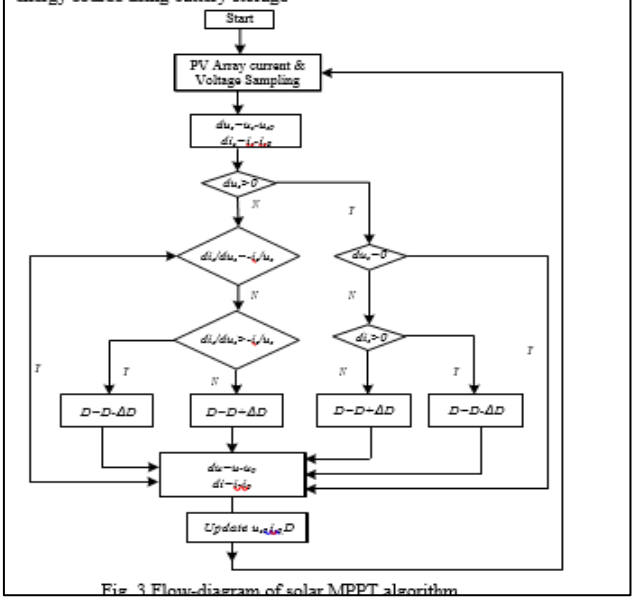

Fig. 3 Flow-diagram of solar MPPT algorithm

IV. RESULTS AND DISCUSSION

The Simulink model of micro-grid fed by REGS is developed in Matlab. The solar panels and wind turbine are modeled using their functions. Fig. 7 shows the performance of the system when the wind generator is taken in an out of the system. Fig. 8 shows the performance of the system when solar PV system is taken in and taken out of the system. Both the above scenarios also discuss the MPPT operation through RSC and solar converter. Fig. 9 shows results at loss of load and Fig. 10 at unbalanced nonlinear load. Fig. 11 shows a scenario when stored energy and generated power are low and external charging requirement through RSC is activated. Fig. 12 shows scenario when DC bus voltage is running at high charging power.

A. Performance of System at Constant Load and Cut-in and Cut-out of Wind Power.

As shown in Fig. 7, the system is started with 10 kW and 6 kVAR load without wind or solar energy sources. At t=2.25 s, the wind generator at wind speed of 7 m/s, is taken in service. As a result, a momentary fluctuation in the system voltage is observed. At t=6.0 s, the wind speed of turbine is increased from 7 m/s to 8 m/s followed by reduction of the wind speed to its original value at t=10.0 s. The rotor control action, maintains the desired rotational speed as per the W-MPPT algorithm. At t=14 s, the wind generator is taken out of service.

During cut-in and cutout of wind generator, momentary, the voltage surge is observed. The duration and magnitude of the voltage surge, are within an IEEE 1547 standard.

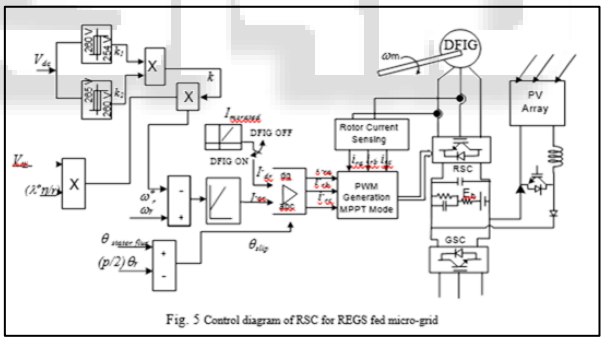

Fig. 5 Control diagram of RSC for REGS fed micro-grid

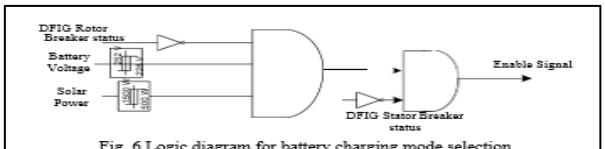

Fig. 6 Logic diagram for battery charging mode selection.

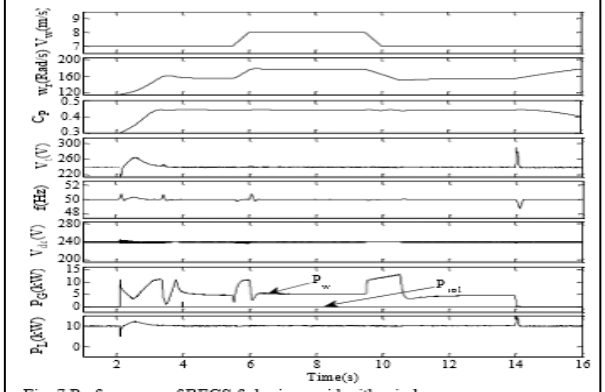

Fig. 7 Performance of REGS fed micro-grid with wind energy source

B. Performance of System at Constant Load and Cut-in and Cut-out of Solar Power

The system is started with a 10 kW and 6 kVAR load without wind or solar energy. As shown in Fig. 8, at t=2.25 s, solar system is taken into the service at radiation of 800 W/m^2. At t=4 s, the solar radiation is raised to 900 W/m^2 and again it is reduced to 800 W/m^2 at t=6 s. The solar converter adjusts the solar PV voltage and operates at S-MPPT. At t=7 s, the solar system is taken out of service. No significant variation of system voltage is observed at any transition point.

C. Performance of System at Unbalanced Nonlinear Load

The performance of the system at unbalanced nonlinear is shown in Fig. 9. A micro-grid should be suitable to provide requirement of unbalanced nonlinear load. A worst case scenario is taken when there are no generating sources. The connected load consists of 2 kW linear load and 8 kW nonlinear load. At t=3.25 s, the load of a-phase is disconnected from the network followed by b-phase load at t=3.46 s. It is seen from the results that the system is able to provide quality power to its customer in case of unbalanced as well as nonlinear load.

D. Performance of System at Loss of Load

The performance of the micro-grid for loss of load, is shown in Fig. 10. A 10 kW and 6 kVAR load, is connected at the terminals prior to start of simulation. Neither wind nor solar power, is available and the load is fed by the battery. At t=2 s, the system load is disconnected. It is found that the system voltage and frequency remain constant of the network.

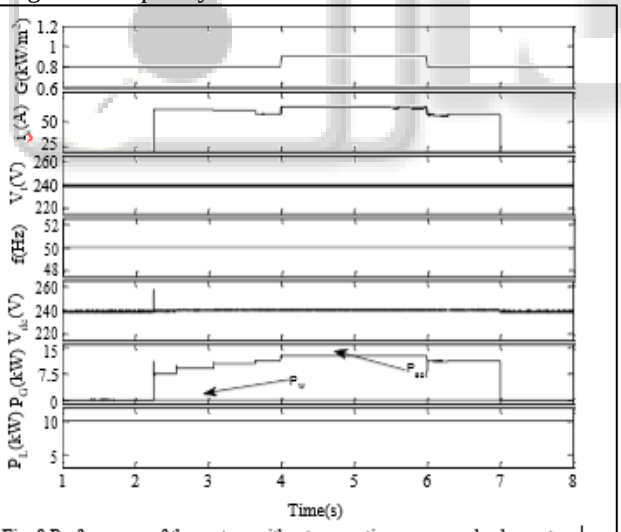

Fig. 8 Performance of the system without generating source and solar system is taken in the service.

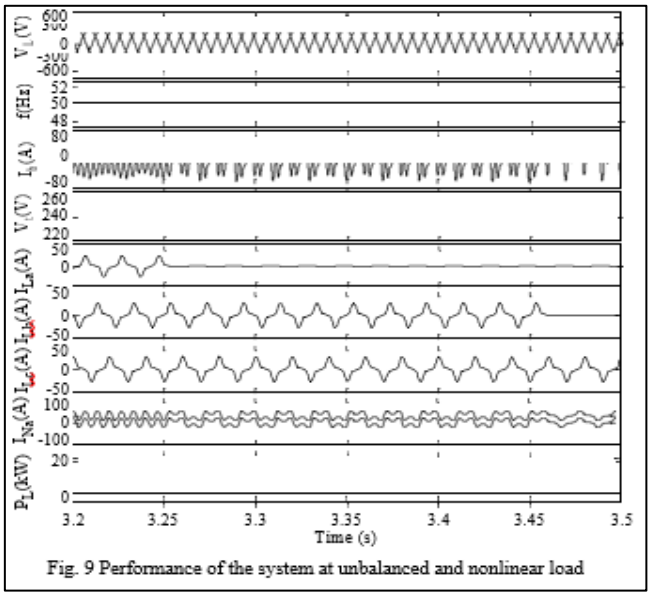

Fig. 9 Performance of the system at unbalanced and nonlinear load

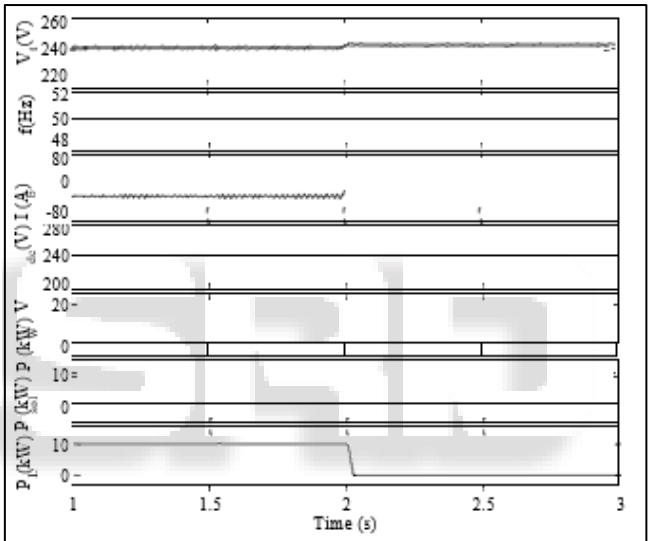

Fig.10 Performance of the system under loss of load at battery power

E. System Running without Generating Source and Battery Charged from the Grid

Fig. 11 shows the scenario when there are no generating sources feeding to the network combined with low battery. External charging is required to sustain the load requirement. Charging circuit is enabled as per the logic diagram of Fig. 6. At t=4 s, wind generation is taken out of service and because of lower battery voltage, the charging circuit is initiated. As a result external power is injected through the RSC to cater load requirement in addition to charging the batteries.

F. Performance of System during High Generation and Over- voltage Scenario of DC bus

Performance of system at high net generation and over-voltage scenario of DC bus, is shown in Fig. 12. To make the effect visible, the AH of the battery is reduced by 1/200 times. The wind speed and solar irradiance, are kept 9 m/s and 700 W/m^2 respectively. It is seen from the curve, that once the V_{dc} reaches 260 V, RSC control reduces the DFIG speed set point to 85% of the MPPT set point. It is seen

from Fig. 12 that charging power, P_c is reduced and the voltage rise is reduced.

V. EXPERIMENTAL RESULTS

The proposed micro-grid system is realised in the laboratory using a 3.7 kW wound rotor induction machine as DFIG powered by a DC shunt motor. The solar energy system consists of a solar PV array simulator of a capacity 5 kW. The DC motor with intelligent torque control through buck converter, helps in achieving the wind turbine characteristics. The technical details of the wound rotor induction machine used as DFIG and DC motor used in these experiments, are given in Appendix-B and Appendix-C, respectively. Two numbers of 25 A IGBTs (Insulated Gate Bipolar Transistors) based VSCs (Semikron Make), are used as LSC and RSC. A set of 40 numbers of 12 V, 7 AH seal maintenance free batteries, are arranged in two parallel circuits to attain 240 V at the DC bus of VSCs. A digital controller (DS 1103 R&D) provides switching signals to all converters. The stator terminals of DFIG, are connected to the LSC through a zig- zag transformer. The generator speed is sensed using an encoder and the view of the complete experimental system is shown in Fig. 13. Fig 14(a) shows the experimental results for

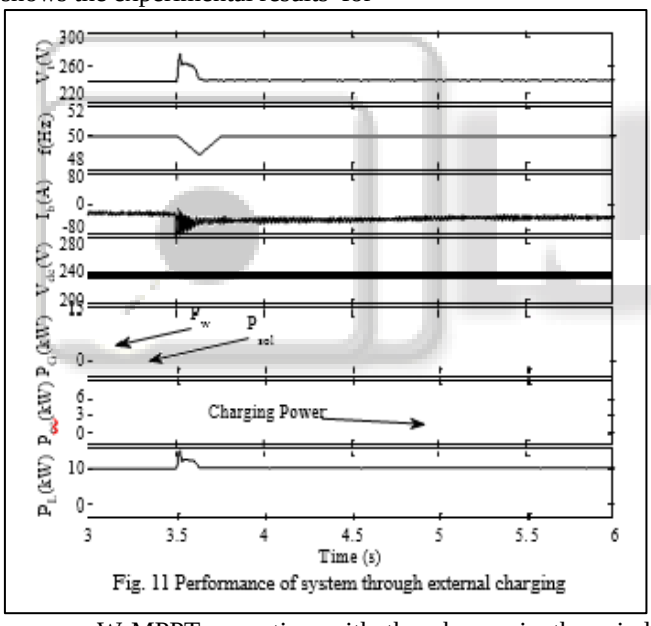

Fig. 11 Performance of system through external charging

W-MPPT operation with the change in the wind speed. Fig. 14(b) shows S-MPPT with the change in the solar radiation. Fig. 15 shows the steady state values of electrical quantities and their harmonic spectra. Fig. 16 show test results when the micro-grid is without the wind power source and the load followed by the connection and disconnection of the load to the grid. Figs. 17 and 18 shows test results for the wind generator disconnection and the reconnection to the micro- grid, respectively. These test results demonstrate the satisfactory operation of the proposed micro-grid under different operating conditions.

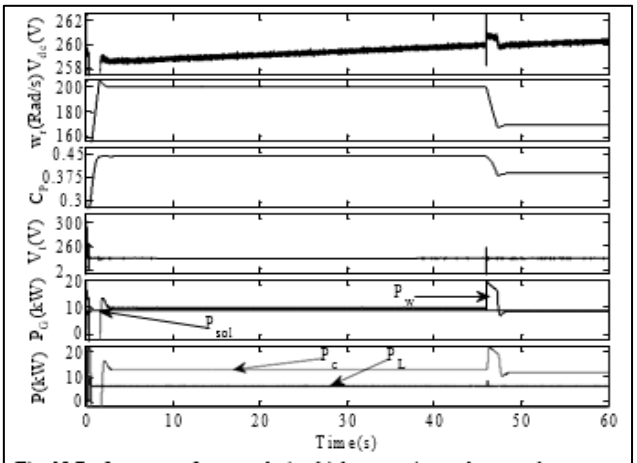

Fig. 12 Performance of system during high generation and over-voltage scenario of DC bus

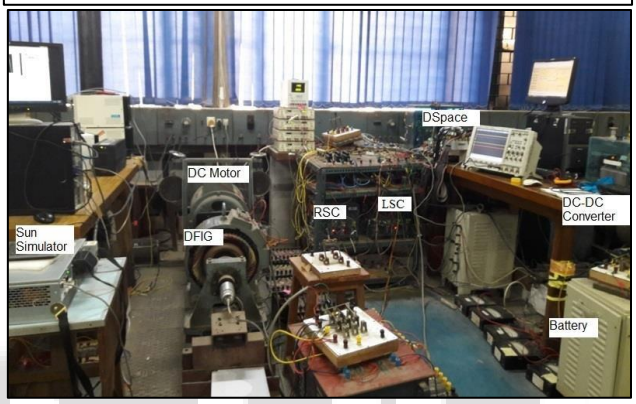

Fig. 13: View of the experimental prototype

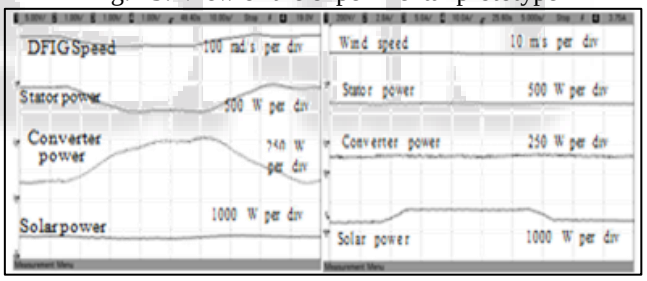

(a) (b)

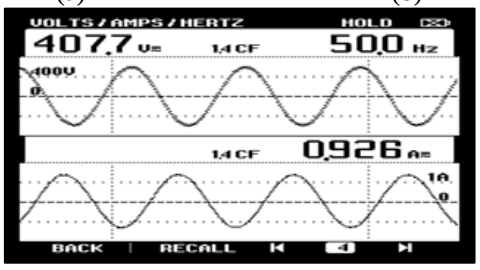

(a)

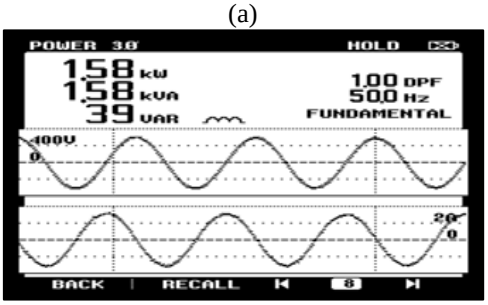

(b)

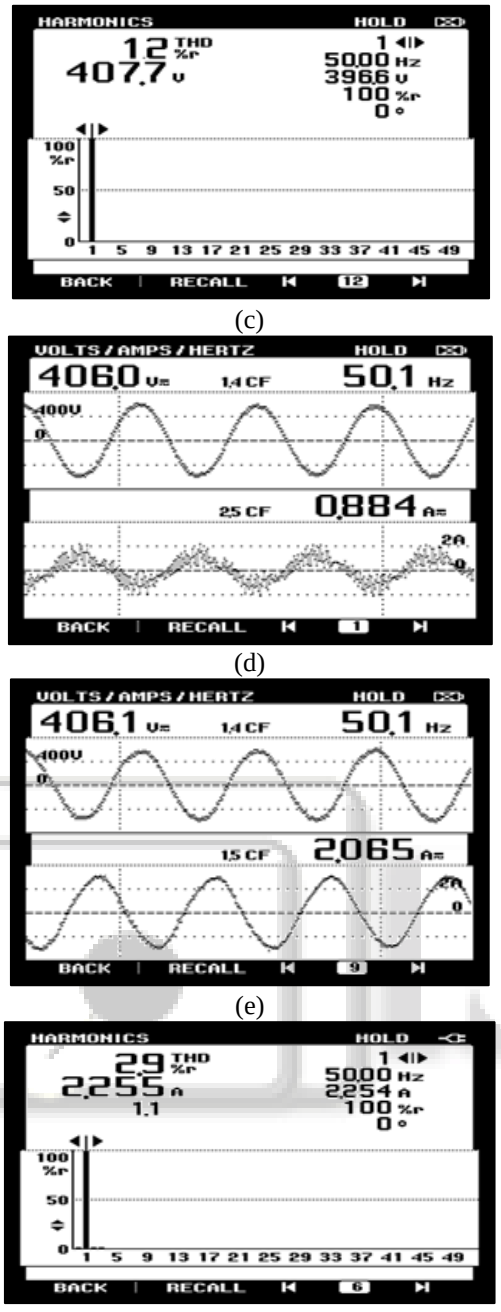

Fig. 15: Test results at steady state (a) i_{La} vs v_{ab}, (b) power at DFIG stator terminal, (c) Harmonic spectrum of v_{ab}, (d) LSC current, (e) i_{sa} vs v_{ab}, (f) harmonic spectrum of i_{sa}

VI. Conclusion

The proposed micro-grid gadget fed from REGS has been observed appropriate for meeting load requirement of a far flung isolated location comprising few households. REGS incorporates of wind and sun strength blocks, which are designed to extract the most energy from the renewable strength sources and at the same time, it presents fine energy to the customers. The system has been designed for entire computerized operation. This paintings also affords the sizing of the important components. The overall performance of the machine has been presented for change in enter conditions for one-of-a-kind sort of load profiles. Under all of the conditions, the strength first-rate on the load terminals, remains inside ideal restrict. The effectiveness of the gadget is also presented with test outcomes with prototype inside the laboratory. The gadget has also envisaged the outside battery charging by using the rotor side converter and its sensors for achieving rectifier operation at unity electricity element.

References

[1] T. Hirose and H. Matsuo, "Standalone Hybrid Wind-Solar Power Generation System Applying Dump Power Control Without Dump Load," IEEE Trans. Industrial Electronics, vol. 59, no. 2, pp. 988-997, Feb. 2012.

[2] Z. Qi, "Coordinated Control for Independent Wind-Solar Hybrid Power System," 2012 Asia-Pacific Power and Energy Engineering Conference, Shanghai, 2012, pp. 1-4.

[3] M. Rezkallah, S. Sharma, A. Chandra and B. Singh, "Implementation and control of small-scale hybrid standalone power generation system employing wind and solar energy," 2016 IEEE Industry Applications Society Annual Meeting, Portland, OR, 2016, pp. 1-7.

[4] A. Hamadi, S. Rahmani, K. Addoweesh and K. Al-Haddad, "A modeling and control of DFIG wind and PV solar energy source generation feeding four wire isolated load," IECON 2013 - 39th Annual Conference of the IEEE Industrial Electronics Society, Vienna, 2013, pp. 7778-7783.

[5] S. K. Tiwari, B. Singh and P. K. Goel, "Design and control of autonomous wind-solar energy system with DFIG feeding 3-phase 4- wire network," 2015 Annual IEEE India Conference (INDICON), New Delhi, 2015, pp. 1-6.

[6] S. K. Tiwari, B. Singh and P. K. Goel, "Design and control of micro- grid fed by renewable energy generating sources," 2016 IEEE 6th Inter. Conference on Power Systems (ICPS), New Delhi, 2016, pp. 1-6.

[7] H. Polinder, F. F. A. van der Pijl, G. J. de Vilder and P. Tavner, "Comparison of direct-drive and geared generator concepts for wind turbines," IEEE International Conference on Electric Machines and Drives, 2005., San Antonio, TX, 2005, pp. 543-550.

[8] Emmanouil A. Bakirtzis and Charis Demoulias "Control of a micro-grid supplied by renewable energy sources and storage batteries," XXth Inter. Conf. on Electrical Machines (ICEM), pp. 2053-2059, 2-5 Sept. 2012.

[9] S. Heier, Grid Integration of Wind Energy Conversion Systems. Hoboken,NJ: Wiley, 1998.

[10] Z.M. Salameh, M.A. Casacca and W.A. Lynch, "A mathematical model for lead-acid batteries," IEEE Trans. Energy Convers., vol. 7, no. 1, pp. 93-97, Mar.1992.

[11] A B. Rey-Boué, R García-Valverde, F de A. Ruz-Vila and José M. Torrelo-Ponce, "An integrative approach to the design methodology for 3-phase power conditioners in Photovoltaic Grid-Connected systems," Energy Conversion and Management, vol. 56, pp. 80–95, Dec 2011.

[12] Z Xuesong,Song Daichun,Ma Youjie and Cheng Deshu, "The simulation and design for MPPT of PV system

based on incremental conductance method," 2010 WASE Inter. Conf. on Information Engineering, Aug, 2010, pp.314 –317.

[13] Shailendra. Kr. Tiwari, B. Singh and P. K. Goel, "Design and Control of Autonomous Wind-Solar Hybrid System with DFIG Feeding a 3-Phase 4-Wire System," in IEEE Transactions on Industry Applications, vol. PP, no. 99, pp. 1-1.

